Measurement of the relative fraction of the gluon-gluon fusion in top-antitop production process at 1.96 TeV proton-antiproton collisions using CDF

N.Kimura
Department of Pure and Applied Sciences,
University of Tsukuba, Japan

We present the measurement of the relative fraction of the subprocess where the initial states are gluon-gluon pairs or quark-antiquark pairs in top-antitop production at 1.96 TeV proton-antiproton collisions. We identify and reconstruct the signal using events which include two high-momentum leptons, and we distinguish the two subproceses by utilizing the correlated spin states of top and antitop quarks. The analysis is based on 2.0 fb^{-1} of data collected with the Collider Detector at Fermilab (CDF) at the Fermilab Tevatron between March 2002 and May 2007. We find the fraction of the gluon-gluon fusion subprocess to be Fgg=$0.53^{+0.36}_{-0.38}$. That is in agreement with the next-to-leading order calculations of Fgg=0.15 ± 0.05.

1 Introduction

In $p\bar{p}$ collisions at $\sqrt{s} = 1.96$ TeV, $t\bar{t}$ pairs are produced dominantly through $q\bar{q}$ annihilation, while about 15% of $t\bar{t}$ pairs are predicted to be produced via gluon-fusion [1]. Because of uncertainties in the large-x gluon luminosity, the prediction of this fraction has a large ambiguity and will change by up to a factor of 2 (from 10% to 20%). Hence, measurement of the gluon fusion fraction will give the knowledge of the gluon content of the proton at large values of x as well as test for the perturbative QCD calculation of gluon fusion.

$t\bar{t}$ pair produced via gluon fusion has a different spin state from one via $q\bar{q}$ annihilation. This difference manifests itself efficiently as an azimuthal correlation of charged leptons in the $t\bar{t}$ dilepton channel [2]. If we assume $t\bar{t}$ pair production close to threshold, $t\bar{t}$ pair produced via gluon fusion and $q\bar{q}$ annihilation is in the following spin state [3]:

$$\begin{aligned} gg &: \quad J = 0, J_z = 0 \\ q\bar{q} &: \quad J = 1, J_z = \pm 1 \ , \end{aligned}$$

where z denotes the initial parton direction (i.e. nearly the beam direction).

Therefore, in the case of gluon fusion, the top quark and the anti-top quark tend to have the opposite spin on any quantize axis, while the aligned spin on the beam axis in the case of $q\bar{q}$ annihilation.

We utilize the difference in azimuthal correlation of charged leptons in the $t\bar{t}$ dilepton channel to distinguish $t\bar{t}$ pair produced via gluon fusion from $q\bar{q}$ annihilation.

2 Data Sample & Event Selection & Background Table

This analysis is based on an integrated luminosity of 2.0 fb^{-1} collected with the CDFII detector[5] between March 2002 and March 2007. The data are collected with an inclusive high P$_T$ lepton trigger. The event signature of $t\bar{t}$ dilepton events is that the event has two high p_T leptons from W decay, large missing E_T due to two missing neutrinos, and two jets originating from b-quarks. We require more then 20 GeV two lepton, more than 25 GeV Missing E$_T$ and some background reduction cut like a Z mass region veto. We observe 145 $t\bar{t}$ candidate events with an expected background of 49.5 events. The dominant background processes remained by DIL selection are diboson production ($WW/WZ/ZZ$), Drell-Yan ($q\bar{q} \to Z^*/\gamma \to ee, \mu\mu, \tau\tau$), and W+jets production where one jet is misidentified as a lepton.

3 Signal and Background templates

The strategy of the gluon fusion measurement is that we fit composition of expected $\Delta\phi$ distribution of gg, $q\bar{q}$, and background with one of data supposing gg fraction as a free fit parameter. Therefore, we introduce the expected $\Delta\phi$ distributions (templates) of gg, $q\bar{q}$, and each background process in this section.

3.1 Gluon fusion and $q\bar{q}$ annihilation

To obtain Δphi in the gluon fusion and $q\bar{q}$ annihilation, we use $t\bar{t}$ pair production Monte Carlo simulation sample which is generated by HERWIG[7] event generator and CDF detector simulator with top quark mass $M_t = 175\ GeV$. In this simulation sample, CTEQ5L set is used as the parton distribution function of proton and anti-proton, and we find about 5% of the sample comes from gluon fusion and the rest comes from $q\bar{q}$ annihilation according to initial state partons.

We separate $t\bar{t}$ events via gluon fusion from $q\bar{q}$ annihilation, and obtain $\Delta\phi$ distributions of gg and $q\bar{q}$ events after DIL selection, separately. Figure 1 shows the distributions of gg (right) and $q\bar{q}$ (left). The histograms are fitted with the following function:

$$\mathcal{F}_i = (3 - P_i^0 cos(\Delta\phi) + P_i^1 cos(2\Delta\phi) + P_i^2 cos(3\Delta\phi))/3\pi, \tag{1}$$

where $P_i^{(n)}$s indicate fitting parameters and the suffix i represent the process, i.e. $i = gg, q\bar{q}$ here. We adopt the function composed with cosine since $\Delta\phi$ distribution should be periodic. The solid curve in the figure indicate the best fit results.

3.2 Background

We make $\Delta\phi$ distribution of each background process separately. For diboson (WW, WZ, and ZZ) events and $Z \to \tau\tau$ events, we rely on MC simulation samples which are generated with PYTHIA[6] event generator. For Drell-Yan ($Z \to ee, \mu\mu$) events, we also rely on MC simulation samples, but which are generated with Alpgen event generator. For $W\gamma$ events, we ignore the background from this process, since the contribution from $W\gamma$ to background are negligibly small. For fake events, i.e. one lepton with jets events where one of jets is misidentified as

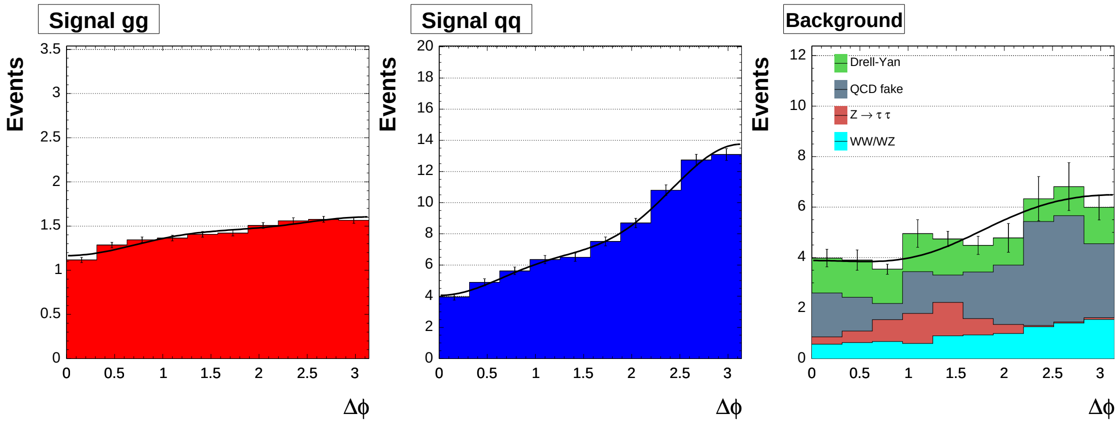

Figure 1: The distributions of $\Delta\phi$ of gluon fusion (left), $q\bar{q}$ annihilation (center) and background(right). The total number in each histogram is normalized to expectation assuming 6.7 pb $t\bar{t}$ cross section. The error bars originate from Monte Carlo statistics. The solid curves in the figure indicate the fit results.

another lepton, we use a real event which contains a lepton and at least one "fakeable" jet and make one of the jets in an events forcibly to be mis-reconstructed as an electron or a muon. In this case, the event weight is not unit, but is adopted to be their fake rate. We fit the distribution to Eqn. (1).

4 Determination of gg Fraction

We define an unbinned likelihood as follows:

$$\begin{aligned} \mathcal{L}(\mathcal{F}_{gg}, n_{\rm s}) &\equiv \prod_i \frac{n_{\rm s} f_{t\bar{t}}(\Delta\phi_i; \mathcal{F}_{gg}) + n_{\rm b} f_{\rm b}(\Delta\phi_i)}{n_{\rm s} + n_{\rm b}} \\ f_{t\bar{t}}(\Delta\phi_i; \mathcal{F}_{gg}) &\equiv \frac{\mathcal{F}_{gg} f_{gg}(\Delta\phi_i) + (1-\mathcal{F}_{gg}) f_{q\bar{q}}(\Delta\phi_i)}{\mathcal{F}_{gg} + (1-\mathcal{F}_{gg})} , \end{aligned}$$

where $\mathcal{F}_{gg}$ and $n_{\rm s}$ are assumed gg fraction and number of $t\bar{t}$ events, respectively. $\Delta\phi_i$ denotes $\Delta\phi$ observed in the i-th candidate event. N is the total number of candidate events, and $n_{\rm b}$ indicates the expected number of background events. The functions f_{gg}, $f_{q\bar{q}}$, and $f_{\rm b}$ are probability density of $\Delta\phi$ for gg, $q\bar{q}$, and background events, which are obtained in Sec.3, respectively. We take $\mathcal{F}_{gg}$ which maximizes this likelihood as the observed gg fraction, and describe this as $\mathcal{F}_{gg}^{\rm measured}$ hereafter.

5 Systematic Uncertainties

We discuss here about possible systematic uncertainties and integrate them into F-C confidence belt. We consider the systematics source of Shapes of $\Delta\phi$ templates and Expected number of background, Acceptance ratio of gg to $q\bar{q}$, Estimation method of systematic uncertainty, Theoretical calculation of $t\bar{t}$ pair production matrix element, Initial/Final state radiation and Parton distribution function.

6 Result

Finally, we reveal $\Delta\phi$ distribution of the data sample after we fixed the analysis method and studies of systematic uncertainties.

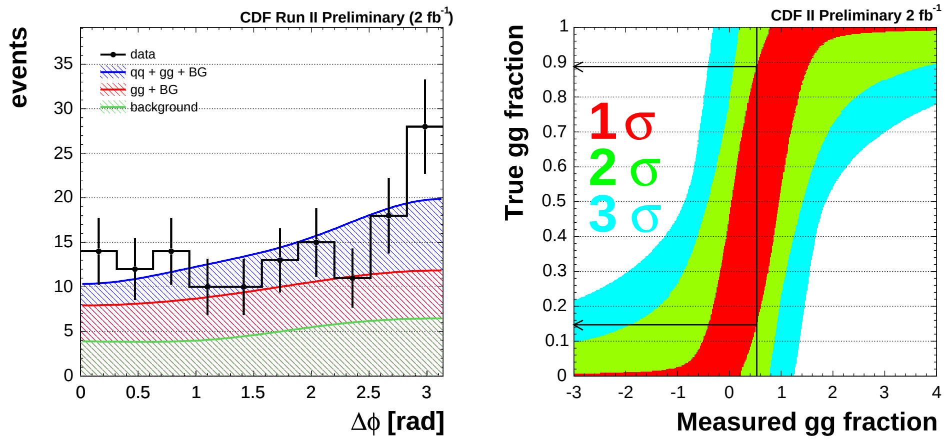

Figure 2: The distribution of $\Delta\phi$ in 2.0 fb^{-1} data (left). The solid curve on the histogram means the best fit. The solid line on the confidence belt (right) indicates $\mathcal{F}_{gg}^{\text{measured}}$ and its cross section with the confidence belt corresponds to the confidence interval on $\mathcal{F}_{gg}^{\text{true}}$.

Figure 2 indicates the distribution of $\Delta\phi$ in 2.0 fb^{-1} data (left). The solid curve on the histogram means the best fit. The solid line on the confidence belt (right) indicates $\mathcal{F}_{gg}^{\text{measured}}$ and its cross section with the confidence belt corresponds to the confidence interval on $\mathcal{F}_{gg}^{\text{true}}$. From this, we retrieve the following results:

$$\mathcal{F}_{gg} \quad = \quad 0.53\ ^{+0.36}_{-0.38}\ \left(^{+0.35}_{-0.37}(stat.)^{+0.07}_{-0.08}(+syst.)\right) \tag{2}$$

Acknowledgments

We thank the Fermilab staff and the technical staffs of the participating institutions for their vital contributions.

References

1. N. Kidonakis et al., Phys, Rev. D **68** 2003 114014; M. Cacciari et al., J.High Energy Phys. **0404** 2004 068
2. T. Arens, et al., Phys, Lett. B **302** 1993 501-506
3. Y. Hara, Prog, Theor. Phys. **86** 1991 779
4. D.Acosta et al., Phys, Rev, Lett. **93** 142001 (2004)
5. F. Abe, et al., Nucl. Instrum. Methods Phys. Res. A **271**, 387 (1988); D. Amidei, et al., Nucl. Instum. Methods Phys. Res. A **350**, 73 (1994); F. Abe, et al., Phys. Rev. D **52**, 4784 (1995); P. Azzi, et al., Nucl. Instrum. Methods Phys. Res. A **360**, 137 (1995); The CDFII Detector Technical Design Report, Fermilab-Pub-96/390-E
6. T. Sjostrand et al., High-Energy-Physics Event Generation with PYTHIA 6.1, Comput. Phys. Commun. **135**, 238 (2001).
7. G. Corcella et al., HERWIG 6: An Event Generator for Hadron Emission Reactions with Interfering Gluons (including supersymmetric processes), JHEP **01**, 10 (2001).